Research Square

Preprints are preliminary reports that have not undergone peer review.
They should not be considered conclusive, used to inform clinical practice,
or referenced by the media as validated information.

Seasonal herding distinguishes Kura–Araxes and local communities in the Early Bronze Age Levant

Gwendoline Maurer

maurerg@cardiff.ac.uk

University College London

Rafi Greenberg

Tel Aviv University

Delphine Frémondeau

University College London

Alexandra Nederbragt

Cardiff University

Rhiannon E. Stevens

University College London

Research Article

Keywords:

Posted Date: November 12th, 2026

DOI: https://doi.org/10.21203/rs.3.rs-11521935/v1

License: This work is licensed under a Creative Commons Attribution 4.0 International License.
Read Full License

Additional Declarations: No competing interests reported.

Seasonal herding distinguishes Kura–Araxes and local communities in the Early Bronze Age Levant

Gwendoline Maurer[1,2]*, Rafi Greenberg[3]*, Delphine Frémondeau[1], Alexandra Nederbragt[4] & Rhiannon E. Stevens[1]

[1]Institute of Archaeology, University College London, London, United Kingdom

[2]Department of Archaeology and Conservation, School of Global Humanities, Cardiff University, Cardiff, United Kingdom

[3]Institute of Archaeology, Tel Aviv University, Tel Aviv, Israel

[4]School of Physical, Chemical, and Environmental Sciences, Cardiff University, Cardiff, United Kingdom

***Corresponding authors: maurerg@cardiff.ac.uk; grafi@tauex.tau.ac.il**

ABSTRACT

The Kura–Araxes tradition, originating in the southern Caucasus, spread across much of Southwest Asia during the Early Bronze Age, reaching as far south as the Levant. There, Khirbet Kerak Ware (KKW; c. 2850–2500 BCE) communities lived alongside local populations, but how far they were integrated into Levantine society remains debated. Seasonal herd management, linked to land access and agricultural scheduling, is a sensitive proxy for such integration. At Tel Bet Yerah (Khirbet el-Kerak), KKW and local neighbourhoods coexisted within one town, making it an ideal test case. We present the first sequential $\delta^{18}O$ and $\delta^{13}C$ analyses of livestock directly associated with KKW in the Levant. We demonstrate a marked divergence: local Levantine herding was integrated into a Mediterranean agropastoral cycle, whereas KKW herding operated largely outside it, some herds moving seasonally into steppe environments. The two communities maintained distinct agropastoral and land-use practices, refining models of Kura–Araxes spread into the Levant.

"Khirbet Kerak" Culture

Long defined by its distinctive ceramics (Khirbet Kerak Ware, KKW) as the southernmost expression of the Kura–Araxes culture of the southern Caucasus and eastern Anatolia [1,2], the Khirbet Kerak phenomenon in the Levant is now known to comprise a set of spatial, material and bio-archaeological dispositions evidenced at scores of sites extending from the Amuq valley in western Syria to the northern Jordan valley and its flanks [3,4].

In the southern Levant, while the presence of KKW has been documented widely, the presence of a sizable community of KKW producers and consumers is confined to seven or eight sites [5] (Fig. 1) with stratified sequences that anchor the chronology [6–10].
The degree to which KKW reflects migration linked to Transcaucasia or local interaction and hybridisation has long been debated [7,11–14]. Petrographic and chaîne opératoire studies show local production using indigenous clays but conservative, non-local technologies, challenging simple migration or diffusion models [15,16].

Tel Bet Yerah, a 30 ha mound on the southern shore of the Sea of Galilee, uniquely preserves large, stratified and contemporaneous KKW-associated (henceforth, KKW) and local-tradition (henceforth, local) habitation areas within a fortified town with an urban grid, albeit a patchy one [17,18]. In the principal excavated area in the north part of the mound, KKW

occupation was excavated mainly within the abandoned foundations of the large public 'Circles Building' and in the open area ('plaza') to its north (excavation fields SA-M, GB-H), while a local sequence (excavation field SA-S) extending from late EB I to EB III was excavated along the paved road flanking the Circles Building on the west [11,19]. Bayesian chronology confirms that KKW contexts and proximate local compounds were coeval in the EB III [20], making the site ideal for testing whether cultural distinctions extended to pastoral management. Beyond the study of the composition of the herds associated with each group [21,22], the study of sequential stable oxygen and carbon isotopes in sheep, goat and cattle enamel from Tel Bet Yerah provides insight into seasonal herding practices, allowing us to compare both KKW and local Early Bronze Age III herding systems, as well as KKW and Kura Araxes complexes outside the Levant (Fig. 2).

Levantine environmental context

Tel Bet Yerah (Khirbet el-Kerak) lies ~200 m below sea level in the Jordan Valley, within a region of marked topographic and ecological variation (Supplementary Fig. S1a–d). Tel Bet Yerah lies within the wetter Mediterranean zone, together with fertile lowlands such as the Jordan, Hula and Jezreel valleys; in Supplementary Fig. S1b, this zone is represented by forest and maquis, Mediterranean savannoid, batha and garigue, and tragacanthic vegetation. Hereafter, this ecological area is referred to as the Mediterranean zone. Eastwards and South-eastwards, these communities give way to transitional and steppe vegetation and the Badiya, with desert environments extending farther south and southeast [23] (Supplementary Fig. S1b).

The Mediterranean zone is characterised by mild, wet winters, hot, dry summers and predominantly winter precipitation; snow persists at higher elevations in the Lebanon and Anti-Lebanon and occurs episodically across surrounding uplands [24,25] (Supplementary Fig. S1d). These eastward and southward gradients from Mediterranean to increasingly arid steppe and desert environments are also reflected in the distribution of C_3 and C_4 plants. (Supplementary Table S2a).

C_3 and C_4 plants use different photosynthetic pathways and occupy distinct ecological niches, with C_3 plants including trees, shrubs and cool-season grasses and C_4 plants dominated by warm-season grasses, sedges and herbaceous eudicots; their relative distributions are strongly influenced by temperature, growing season and aridity [26,27].

Vegetation in the Mediterranean zone is dominated by C_3 taxa, with C_4 plants occurring patchily where summer moisture or shallow water tables permit (Supplementary Table S2a;

Supplementary Fig. S1b). Around Tel Bet Yerah, vegetation is overwhelmingly C_3, with limited C_4 grasses and *Cyperus* spp. largely confined to wetland margins and of low palatability. C_4 taxa become more common in the increasingly arid transitional steppe (Supplementary Fig. S1b), steppe environments (Supplementary Fig. S1b) to the east, southeast and south, as well as in saline and sandy habitats. The C_4 plant *Noae mucronata* has also been identified in the high altitudes of Mount Hermon [28–34] (Supplementary Fig. S1b and Supplementary Table S2a).

Levantine isotopic context

Enamel $\delta^{18}O$ in livestock reflects the isotopic composition of ingested water, derived from both drinking water and plant water [35]. Animals that obtain a greater proportion of their water from plants can show higher $\delta^{18}O$ values because leaf water becomes enriched in ^{18}O through evaporation [36]. In the Levant, precipitation $\delta^{18}O$ varies seasonally and geographically in response to climate and topography, with wetter conditions generally producing lower, more negative values [37–41]. At Tel Bet Yerah, modelled precipitation $\delta^{18}O$ values range from –6.4‰ in winter to +1.0‰ in summer [40]. Freshwater sources across the region (Supplementary Fig. S1c) broadly reflect precipitation inputs but can be modified by processes such as snowmelt and evaporation [42,43]. Lake Tiberias shows relatively limited variation, ranging from 0 to –2.5‰ VSMOW, whereas ephemeral water sources may become substantially more enriched through evaporation [44,45] (Supplementary Table S2d). Groundwater is generally more negative in $\delta^{18}O$ and less seasonally variable [46]. Consequently, sequential enamel $\delta^{18}O$ can track seasonal variation and changes in water-source use by livestock.

Enamel $\delta^{13}C$ provides a complementary record of seasonal diet and vegetation use. It primarily reflects the relative contribution of C_3 and C_4 vegetation to the diet of livestock [26], although plant $\delta^{13}C$ is also affected by environmental conditions, particularly water stress, humidity and elevation [47–51]. In the Levant, C_3 plants sampled during the wet season (October–April) average –27.27 ± 1.25‰, compared with –25.90 ± 1.52‰ during the dry season (May–September), reflecting the influence of seasonal water availability on C_3 plant $\delta^{13}C$ values [50] (Supplementary Table S2b). C_4 plants in our compiled dataset average –12.81 ± 1.15‰ and range from –14.14‰ to –9.70‰ [52] (Supplementary Table S2b). These differences provide the basis for distinguishing seasonal shifts in C_3 and C_4 consumption, while accounting for variation in C_3 plant $\delta^{13}C$ caused by water stress.

Results

Caprines

The full sequential stable isotope dataset is provided in Supplementary Data S3, with specimen-level summary statistics presented in Table 1. Due to limited sample size, EB II Middle, EB II Latest and EB III Local specimens are treated as a single Local group. It should be noted that only the EB III Local specimens are contemporary with the KKW specimens (Fig. 1).

Caprine enamel $\delta^{18}O$ values range from −1.7‰ to 8.1‰, with intra-tooth amplitudes of 1.3‰–8.4‰ (Table 1). Local caprines (n = 5) range from −0.8‰ to 4.8‰, with amplitudes of 2.2‰–4.3‰ (Supplementary Table S3b). KKW-associated caprines (n = 8) show higher $\delta^{18}O$ values (−1.7‰ to 8.1‰) and a wider range of amplitudes (1.3‰–8.4‰) (Table 1). Among specimens with clearly defined minima and maxima (Fig. 3; KKW n = 6, Local n = 4), there were no significant differences between KKW-associated and Local caprines in $\delta^{18}O$ midpoints (median = 2.53‰ vs 1.53‰; Mann–Whitney U = 6.0, P = 0.26) or intra-tooth amplitudes (median = 5.40‰ vs 3.56‰; U = 8.0, P = 0.48).

Caprine enamel $\delta^{13}C$ values range from −12.3‰ to −5.2‰. Local caprines (n = 5) span −11.5‰ to −6.5‰, with amplitudes of 1.2‰–3.8‰ (Table 1). KKW-associated caprines (n = 8) range from −12.3‰ to −5.2‰, with amplitudes of 1.3‰–5.0‰. Among the same specimens, $\delta^{13}C$ midpoints (median = −9.11‰ vs −9.17‰; U = 10.0, P = 0.76) and intra-tooth amplitudes (median = 2.35‰ vs 2.63‰; U = 11.0, P = 0.91) did not differ significantly between KKW-associated and Local caprines.

Four intra-tooth patterns were identified (Fig. 4): Patterns A–B (KKW) and Patterns C–D (Local), with specimen-level summary statistics presented in Table 1.

Pattern A (TBY70444, TBY70203, TBY70158) shows $\delta^{18}O$ variation, although a distinct minimum is absent in TBY70203. $\delta^{13}C$ is fully sinusoidal only in TBY70444, with absent or weak minima in the other sequences but well-defined maxima throughout and varies in phase with $\delta^{18}O$. $\delta^{13}C$ values indicate a predominantly C_3 diet, with minor C_4 input (~2%) in TBY70158 and seasonal shifts from dry C_3 resources in summer to fresher C_3 resources in winter.

Pattern B (TBY20, TBY70145, TBY70157, TBY70656, TBY702805) shows $\delta^{18}O$ variation, with dampened cycles in TBY70145 and TBY70656, an unclear maximum in TBY70157, and an unclear minimum in TBY20. $\delta^{13}C$ is largely anti-phased with $\delta^{18}O$, indicating summer reliance on dry C_3 resources and increased C_4 intake (~22–38%) during cooler seasons. This pattern records a brief summer C_3 phase followed by prolonged autumn–winter C_4 use. TBY702805 differs slightly, with sinusoidal $\delta^{18}O$ but poorly defined $\delta^{13}C$ optima and alternating phasing, indicating ~18% C_4 intake at the $\delta^{18}O$ minimum and a shift toward a dry, C_3-dominated diet as $\delta^{18}O$ increases.

Pattern C (TBY70647, TBY70489) shows sinusoidal $\delta^{13}C$ variation largely anti-phased with $\delta^{18}O$. $\delta^{18}O$ is sinusoidal in TBY70647 but lacks a clear minimum in TBY70489, and the $\delta^{13}C$ cycle in TBY70647 is dampened (1.2‰). $\delta^{13}C$ minima indicate fresh C_3 intake, whereas higher values reflect drier C_3 resources and modest C_4 input (~16.4%) during cooler seasons.

Pattern D (TBY70168, TBY70652, TBY702839) shows largely anti-phased $\delta^{18}O$–$\delta^{13}C$ variation. In TBY70168 and TBY702839, both isotopes vary sinusoidally, with $\delta^{13}C$ maxima coinciding with $\delta^{18}O$ minima and indicating C_4 intake (~19% and ~13.5%), and minima reflecting dry, C_3-dominated diets. TBY70652 lacks clear optima but shows opposed isotope variation and a shift from higher to lower $\delta^{13}C$ values. Pattern D also shows a diverging $\delta^{18}O$ baseline relative to Pattern B (Fig. 3).

Cattle

Enamel $\delta^{18}O$ values range from −3.9‰ to 4.7‰, with amplitudes (where identifiable) of 1.9‰–3.6‰. KKW cattle (n = 3) range from −1.6‰ to 4.1‰ (1.9‰–3.6‰), while Local cattle (n = 3) range from −3.9‰ to 4.7‰, with a single identifiable amplitude of 1.7‰. Cattle enamel $\delta^{13}C$ values range from −11.5‰ to −6.0‰, with amplitudes of 0.9‰–3.3‰. KKW cattle (n = 3) range from −11.5‰ to −9.3‰ (1.1‰–1.5‰), while Local cattle (n = 3) range from −10.8‰ to −7.9‰ (0.9‰–3.3‰).

Three patterns were identified (Fig. 4): Pattern E (KKW & Local), Pattern F (Local), and Pattern G (Local).

Pattern E (TBY45, TBY70316, TBY37, TBY702849) comprises two sub-patterns. Sub-pattern E.1 (KKW) includes TBY70316 and TBY45: TBY70316 shows sinusoidal $\delta^{18}O$ and $\delta^{13}C$ variation, whereas TBY45 lacks clear periodicity. $\delta^{13}C$ indicates year-round C_3 consumption, with seasonal shifts between fresher winter and drier summer resources. Sub-pattern E.2 (TBY37 (EB II) and TBY702849 (KKW) shows sinusoidal, in-phase $\delta^{18}O$–$\delta^{13}C$

variation, with enriched summer $\delta^{18}O$ values producing larger amplitudes than in other cattle specimens and persistent C_3 consumption throughout.

Pattern F (TBY702827; EB II late) shows sinusoidal $\delta^{18}O$ variation, while $\delta^{13}C$ lacks clear periodicity. Values indicate dry, C_3-dominated intake in summer and recurring increases consistent with substantial C_4 input (up to 29.4%) during cooler seasons.

Pattern G (TBY39; EB III Local) shows weak $\delta^{18}O$ sinusoidality with a poorly defined minimum, while $\delta^{13}C$ exhibits a dampened cycle; the proxies are largely anti-phased. $\delta^{18}O$ is more depleted in summer than winter, indicating a reversal of the expected seasonal signal. $\delta^{13}C$ indicates dry, C_3-dominated intake in summer and fresher C_3 intake in winter.

Seasonality of birth

Modelling results for caprines (n = 6) and cattle (n = 1) are presented in Fig. 5 and Supplementary Table S3c. In caprines, fitted periods (X) range from 22.1 to 30.7 mm, with x_0/X values between 0.27 and 0.71. KKW caprines show values of 0.27–0.62, while local sheep (n = 3) range from 0.45 to 0.71, corresponding to births from late spring to early autumn. The KKW cattle specimen has $x_0/X = 0.26$.

Discussion

Local-horizon isotopic sequences indicate a synchronised agropastoral system structured around seasonal use of C_3-dominated pastures within the Mediterranean zone (Fig. 1; Supplementary Fig. S1b), post-harvest field and orchard grazing, and flexible summer pasture exploitation (Fig. 2).

Across Patterns C, D and F, isotopic signals show a spring–summer emphasis on Mediterranean C_3 vegetation, followed by a brief cooler-season shift introducing brief C_4 input. Locally herded, C_3 -dominated caprines with minor C_4 input are likewise documented at contemporary EB III Tell es-Safi/Gath [53], indicating that comparable practices occurred elsewhere in the southern Levant.

Given the limited availability of C_4 biomass in Mediterranean settings, this enrichment could be consistent with intermittent post-harvest access to cultivated fields and orchard margins, where C_3 residues and ruderal C_4 weeds were available. Livestock can support cultivation through post-harvest grazing, clearing crop residues while manuring fields for the next growing season, a widely documented practice in Mediterranean and Middle Eastern agroecosystems (Fig. 6). Its presence in both cattle and caprines suggests a shared, agro-integrated land-use strategy.

This interpretation is supported by archaeobotanical evidence. Charcoal assemblages indicate that local landscape use was closely tied to olive and fig horticulture, with pruning reflecting sustained orchard management [54]. Two proposed harvest windows (late spring and late summer/autumn) likely enabled field and orchard grazing, producing the brief recurring C_4 signal in local sequences. The Local-horizon assemblage includes disturbance-tolerant C_4 weeds such as *Amaranthus graecizans* and *Portulaca oleracea*, and specifically the absence of *Trifolium* sp., a common C_3 weed, suggesting a deliberate use of low growing weeds as fodder post-harvest [55]. Legumes, fruits, and olives are late-autumn crops, interestingly they are common in local archaeobotanical assemblages and largely absent from KKW contexts [55]. Further, the birthing season of locally associated sheep coincide with or occur shortly after these harvest windows, when field and orchard fodder would have been most available.

Within this agropastoral integrated system, summer pasture use varied. Patterns C and D differ primarily in their summer grazing strategies. In Pattern C, a summer $\delta^{18}O$ dip coincides with a $\delta^{13}C$ minimum, indicating access to isotopically depleted waters, consistent with snowmelt influence and/or higher-elevation water sources, alongside fresh C_3 forage. Comparable values in snowmelt-fed rivers of the Upper Jordan system (e.g. the Hasbani and Banias; Supplementary Fig. S1c)[42] suggest seasonal movement to cooler, wetter higher elevations towards the north, where fresh C_3 forage would have been available during summer. By contrast, Pattern D lacks a summer $\delta^{18}O$ dip and evidence for fresh C_3 intake, indicating summer grazing within lower-elevation Mediterranean settings. Cattle Patterns E.2 and G similarly reflect year-round Mediterranean grazing, with fresh C_3 forage consumed in the wet season and dry or senescent C_3 biomass in summer. In Pattern G, access to isotopically depleted summer waters without a corresponding $\delta^{13}C$ shift suggests use of snowmelt-derived waters i.e. lowland Upper Jordan contexts, rather than further upland pastures.

Given the small sample size, these patterns should be interpreted cautiously, but they suggest dispersed practices in summer, followed by more collectively coordinated autumn–winter management linked to post-harvest field use.

By contrast, KKW-associated herding appears decoupled from local agropastoral cycles, neither coordinated with cultivation schedules nor integrated into post-harvest field use and

follows two distinct pastoral strategies (Fig. 2). Patterns A and E are consistent with year-round Mediterranean C_3 grazing structured around seasonal variation in C_3 forage, rather than agriculturally synchronised grazing. Pattern B shows a prolonged autumn–winter C_4 signal inconsistent with year-round Mediterranean herding, indicating seasonal movement of caprines away from Tel Bet Yerah into mixed C_3/C_4 environments where C_4 resources persist through cooler months. Elevated C_4 intake in southern Levantine caprines has elsewhere been linked to herding beyond local C_3 pastures [56].

This could be consistent with the use of southeasterly and more easterly zones (Fig. 1), where mild winters sustain multiple C_4 taxa i.e. *Noaea mucronata*, a documented sheep winter forage in Levantine steppe environments [57]. Herds move into transitional and steppe zones in late autumn, grazing a mosaic of dried C_3 plants from the previous season alongside winter-tolerant C_4 shrubs and grasses. Winter rains then promote fresh C_3 growth (e.g., *Carex*, *Poa*), while resistant C_4 species continue to contribute to the available pasture. By late spring, as grazing and water availability decline, herds shift back north or westwards into the Mediterranean zone to exploit summer forage dominated by water-stressed C_3 plants.

One possibility is winter–spring access to the lower Jordan Valley (the Ghor; Fig. 1) transitional vegetation (Supplementary Fig. S1b and Supplementary Table S2a), in proximity to known KKW-rich sites such as Tel Yaqush and Tall ash-Shuna, followed by a return north in late spring/early summer. Further, seasonal east–west movement has close parallels in historically documented pastoral practices across the Levant [58], and isotopic evidence suggests steppe or desert grazing in later periods [59,60], but it remains unattested for the Early Bronze Age. While our isotopic data cannot pinpoint a precise location, both southeasterly and easterly scenarios (Fig. 1) provide ecologically plausible mechanisms for producing the prolonged cool-season C_4 signal observed in Pattern B.

Birth seasonality broadly aligns with the mobility framework, though the sample is limited. Livestock births coincide with increased winter steppe pasture and fresh Mediterranean C_3 vegetation, consistent with herding systems that track seasonal forage gradients between steppe and Mediterranean zones.

Archaeobotanical evidence further suggests that these differences extended beyond herding alone. The distribution of *Lolium* species, linked to soil conditions, implies that cultivation was structured across distinct niches, with local populations focusing on Jordan Valley soils and Khirbet Kerak groups exploiting basalt-derived landscapes to the north and east of Tel

Bet Yerah [55]. Basaltic landscapes are widespread across the eastern Lower Galilee, Golan Heights, southern Syria and northeastern Jordan [61–63].

Although the small sample size limits the strength of inference, KKW herding appears less normative, with variability potentially driven by household autonomy, risk-buffering herd division, temporal change, and rainfall-linked shifts in pasture availability.
Herding practices appear weakly integrated into local agropastoral cycles, suggesting that KKW-associated livestock management operated partly outside the crop-livestock economy of Tel Bet Yerah

These differences have broader implications for interpreting Khirbet Kerak Ware communities in the Levant. Winter movement to distant pastures overlaps with the agricultural growing season, particularly for cereals and legumes that begin growth in early winter. Such overlap likely required spatial separation between cultivation and intensive grazing to avoid crop damage and competition over nearby land. In a setting where agricultural intensification and settlement expansion increased pressure on surrounding landscapes during the EB II–III, herding would be expected to shift outward to reduce interference with cultivated fields. Tel Bet Yerah, as a large EB III site (c. 30 ha) situated in a highly productive zone, likely experienced particularly strong pressure on nearby land. Seasonal displacement of KKW flocks, especially in winter, can therefore be understood as a strategic adaptation that reduced overlap with local agro-pastoral scheduling and helped avoid conflict or bottlenecks in land use.
The broader settlement landscape is consistent with the feasibility of such seasonal circuits. EB I–III settlement patterns include both large sites requiring dense landscape use and smaller or potentially seasonal sites in semi-arid steppe margins, suggesting environments where more mobile, flexible herding could be practiced [64]. The presence of Khirbet Kerak Ware at sites along eastern steppe margins (i.e. Khirbet ez-Zeraqun and Khirbet al-Batrawy) and within the Jordan Valley (Fig. 1), including Tel Yaqush in the Ghor, is compatible with movement corridors or recurring seasonal interaction between Tel Bet Yerah and eastern/southern grazing zones.
In the wider Kura–Araxes culture context, our study contributes to a growing body of work, including case studies from Köhne Shahar in Iran and Maxta I in Nakhchivan, that demonstrates patterns of seasonal local horizonal transhumance, highlighting the diversity of Kura–Araxes pastoral practices [65,66].

Methods

Materials

Specimens from Tel Bet Yerah were phased within the site stratigraphy and its Bayesian radiocarbon model, which places the Early Bronze I-II transition in the 32nd century BCE and the Early Bronze II-III transition at about 2850 BCE (ref. [20], fig. 9). They originate from Areas SA-M, SA-S and the Circles Building [67] (for context descriptions, see Supplementary Table S3d). KKW contexts were distinguished by their ceramic assemblage as well as by their use of space, the presence of wattle and daub and burnished floor fragments, the presence of distinctive pot-supports (andirons) and figurines, and other, more subtle differences in material culture [12].

We analysed 21 mandibular molars: 14 caprine second molars (M2) and seven cattle (*Bos*) third molars (M3), comprising 250 sequential samples. Two specimens (TBY70329 – Bos; TBY9990333 – Ovis) had poor reproducibility and were excluded (Supplementary Table S3a).

Caprine crown height and anterior-posterior crown diameter (dap) were recorded following Helmer [68], and K-means clustering of these measurements was used to differentiate distinction between loose first (M1) and second (M2) mandibular molars. Loose cattle (*Bos*) mandibular molars were assigned to tooth position following Jones [69]. Sheep and goat morphological differentiation followed Halstead et al. [70], with ambiguous specimens classified as *Ovis/Capra*. Only teeth with preserved enamel–root junctions and crown height >3 cm were included.

Sequential stable isotope analysis

Cementum was removed from M2 and M3 posterior pillars using a tungsten drill bit. Teeth were cleaned, rinsed, air-dried, and enamel sequentially sampled with 1 mm diamond bits (~4–6 mg per increment). Pre-treatment followed Tornero et al. [71]: 4 h in 0.1 M acetic acid (0.1 ml/mg), five deionised-water rinses, and freeze-drying.

Enamel $\delta^{18}O$ and $\delta^{13}C$ were analysed at the Stable Isotope Facility, Cardiff University, and reported in ‰ relative to VPDB (NBS-19), calibrated using Carrara marble and standards NBS-18 and NBS-19. Samples were measured on a Thermo MAT 253 dual-inlet (Kiel IV), acidified for 5 min at 70 °C; long-term precision is 0.021‰ ($\delta^{13}C$) and 0.032‰ ($\delta^{18}O$).

Sequential isotope analysis targets tooth enamel because it mineralises progressively, preserving a chronological isotopic record [72,73]. Therefore, $\delta^{13}C$ and $\delta^{18}O$ values reflect an integrated signal of dietary and environmental inputs during the mineralisation period [74].

In caprines, M2 crown formation spans ~1–13 months [75–78], while in cattle, M3 spans ~12–24 months [72,79,80]. There is a ~ 6-month delay between enamel formation and isotopic signal incorporation [72,78].

Threshold $\delta^{13}C$ values in tooth enamel

Published Levantine plant $\delta^{13}C$ values for C_3 and C_4 taxa were compiled to derive regional enamel cut-offs for wet-season C_3, dry-season C_3 and C_4 diets [50,52] (Supplementary Tables S2b and S2c). Wet-season and dry-season C_3 values correspond to plants sampled during October–April and May–September, respectively, following Hartman and Danin [50]. The C_4 endmember represents a regional Middle Eastern mean and may not capture the full range of Levantine variability. Enamel $\delta^{13}C$ values were estimated using equation and enrichment factors (ε^*) of +14.1‰ for caprines [81] (Supplementary Table S2b) and +14.5‰ for cattle [82] (Supplementary Table S2c).

Modelling of $\delta^{18}O$ sequences

Birth seasonality was modelled following Balasse et al. [83]; specimens lacking clear sinusoidal patterns or preserved enamel–root junctions were excluded, potentially underrepresenting some birth timings. Birth seasons were inferred using modern caprine reference datasets, noting their predominantly Western European origin [83–88] (D. Frémondeau, unpublished data).

Statistical analysis

Differences between KKW-associated and Local caprines in $\delta^{18}O$ and $\delta^{13}C$ midpoints ((minimum + maximum)/2) and intra-tooth amplitudes (maximum − minimum) were assessed using two-tailed Mann–Whitney U tests (exact P values; $\alpha = 0.05$), selected because of the small sample sizes. Only specimens with clearly defined minima and maxima were included (Fig. 3).

Data availability

The original data presented in the study are openly available in the supplementary material. R codes are accessible on GitHub https://github.com/GwenMaurer-arch/Khirbet-el-Kerak-Sequential-Isotopes

References

1. Amiran, R. Yanik Tepe, Shengavit and the Khirbet Kerak Ware. *Anatol. Stud.* **15,** 165–167 (1965).

2. Greenberg, R. & Goren, Y. Introduction: migrating technologies at the cusp of the Early Bronze Age III. *Tel Aviv* **36,** 129–134 (2009).

3. Palumbi, G. & Chataigner, C. The Kura-Araxes culture from the Caucasus to Iran, Anatolia and the Levant: between unity and diversity. A synthesis. *Paléorient* **40,** 247–260 (2014).

4. Sagona, A. G. *The Archaeology of the Caucasus: From Earliest Settlements to the Iron Age* (Cambridge Univ. Press, 2018).

5. Greenberg, R. Notes on the end of the Kura-Araxes ('Khirbet Kerak') presence in the southern Levant in *The Chrono-Cultural Aspect of the EB/MB Transition in the South Caucasus* (eds Badalyan, R. & Perello, B.) 319–330 (Brepols, 2024).

6. Ben-Tor, A., Zuckerman, S., Bechar, S. & Sandhaus, D. *Hazor VII: The 1990–2012 Excavations, the Bronze Age* (Israel Exploration Society, 2017).

7. Greenberg, R. Fragments of an anarchic society: Kura-Araxes territorialization in the third millennium BC town at Tel Bet Yerah. *World Archaeol.* **53,** 384–400 (2021).

8. Rotem, Y., Iserlis, M., Höflmayer, F. & Rowan, Y. M. Tel Yaqush—an Early Bronze Age village in the Central Jordan Valley, Israel. *Bull. Am. Sch. Orient. Res.* **381,** 107–144 (2019).

9. Mazar, A. (ed.) *Excavations at Tel Beth-Shean 1989–1996, Vol. IV: The 4th and 3rd Millennia BCE* (Israel Exploration Society, 2012).

10. Baird, D. & Philip, G. Preliminary report on the third (1993) season of excavations at Tell esh-Shuna North. *Levant* **26,** 111–133 (1994).

11. Greenberg, R., Iserlis, M. & Shimelmitz, R. New evidence for the Anatolian origins of 'Khirbet Kerak Ware people' at Tel Bet Yerah (Israel), c. 2800 BC. *Paléorient* **40,** 183–201 (2014).

12. Greenberg, R., Iserlis, M. & Paz, S. Twenty years of Kura-Araxes research at Tel Bet Yerah: what we have learned. *Aramazd: Armen. J. Near East. Stud.* **16,** 166–182 (2022).

13. Philip, G. Complexity and diversity in the southern Levant during the third millennium BC: the evidence of Khirbet Kerak Ware. *J. Mediterr. Archaeol.* **12,** 26–57 (1999).

14. Zaid, S. Khirbet Kerak Ware in the southern Levant: a case of ethnic identity? *Anc. Near East. Stud.* **56,** 215–265 (2019).

15. Iserlis, M. Khirbet Kerak ware at Bet Yerah: segregation and integration through technology. *Tel Aviv* **36,** 181–195 (2009).

16. Medeghini, L. et al. Is Khirbet Kerak Ware from Khirbet al-Batrawy (Jordan) local or imported pottery? *Anal. Methods* **5,** 6622–6630 (2013).

17. Paz, S. & Greenberg, R. Conceiving the city: streets and incipient urbanism at Early Bronze Age Bet Yerah. *J. Mediterr. Archaeol.* **29,** 197–223 (2016).

18. Paz, S. Urban transformations: continuity, change, rehabilitation and decay at Tel Bet Yerah in the Early Bronze III in *New Horizons in the Study of the Early Bronze III and Early Bronze IV in the Levant* (ed. Richard, S.) 234–248 (Eisenbrauns, 2020).

19. Greenberg, R., Paz, S., Wengrow, D. & Iserlis, M. Tel Bet Yerah: hub of the Early Bronze Age Levant. *Near East. Archaeol.* **75,** 88–107 (2012).

20. Regev, J., Paz, S., Greenberg, R. & Boaretto, E. Radiocarbon chronology of the EB I–II and II–III transitions at Tel Bet Yerah, and its implications for the nature of social change in the southern Levant. *Levant* **51,** 54–75 (2019).

21. Berger, A. 'Feeding cities'? Preliminary notes on the provisioning of animal products at Tel Bet Yerah, Israel in *Archaeozoology of the Near East XII: Proceedings of the 12th International Symposium of the ICAZ Archaeozoology of Southwest Asia and Adjacent Areas Working Group* (eds Çakırlar, C., Chahoud, J., Berthon, R. & Pilaar Birch, S.) 13–26 (Barkhuis, 2018).

22. Maurer, G. & Greenberg, R. Cattle drivers from the north? Animal economy of a diasporic Kura-Araxes community at Tel Bet Yerah. *Levant* **54,** 309–330 (2022).

23. Kushnir, Y., Dayan, U., Ziv, B., Morin, E. & Enzel, Y. Climate of the Levant: phenomena and mechanisms in *Quaternary of the Levant: Environments, Climate Change, and Humans* (eds Enzel, Y. & Bar-Yosef, O.) 31–44 (Cambridge Univ. Press, 2017).

24. Torfstein, A. Climate cycles in the southern Levant and their global climatic connections. *Quat. Sci. Rev.* **221,** 105881 (2019).

25. Fayad, A. et al. Snow hydrology in Mediterranean mountain regions: a review. *J. Hydrol.* **551,** 374–396 (2017).

26. Smith, B. & Epstein, S. Two categories of $^{13}C/^{12}C$ ratios for higher plants. *Plant Physiol.* **47,** 380–384 (1971).

27. Ehleringer, J. R., Cerling, T. E. & Helliker, B. R. C_4 photosynthesis, atmospheric CO_2, and climate. *Oecologia* **112,** 285–299 (1997).

28. Abi-Saleh, B. & Safi, S. Carte de la végétation du Liban. *Ecol. Mediterr.* **14,** 123–141 (1988).

29. Al-Eisawi, D. M. *Field Guide to Wild Flowers of Jordan and Neighbouring Countries* (Jordan Press, 1998).

30. Danin, A. Flora and vegetation of Israel and adjacent areas in *The Zoogeography of Israel: The Distribution and Abundance at a Zoogeographical Crossroad* (eds Yom-Tov, Y. & Tchernov, E.) 251–276 (Springer, 1988).

31. Ish-Shalom-Gordon, N. The Mediterranean grazing ecosystems of the Golan Heights. *Agric. Ecosyst. Environ.* **54,** 67–76 (1995).

32. Mouterde, P. *Nouvelle Flore du Liban et de la Syrie* Vol. 1 (Éditions de l'Imprimerie Catholique, 1966).

33. Post, G. E. *Flora of Syria, Palestine and Sinai: A Handbook of the Flowering Plants and Ferns, Native and Naturalized from the Taurus to Ras Muhammad and from the Mediterranean Sea to the Syrian Desert* Vol. 1, 2nd edn (rev. Dinsmore, J. E.) (American Press, 1932).

34. Zohary, M. *Plant Life of Palestine: Israel and Jordan* (Ronald Press, 1962).

35. Bryant, D. & Froelich, P. A model of oxygen isotope fractionation in body water of large mammals. *Geochim. Cosmochim. Acta* **59,** 4523–4537 (1995).

36. Barbour, M., Roden, J., Farquhar, G. & Ehleringer, J. Expressing leaf water and cellulose oxygen isotope ratios as enrichment above source water reveals evidence of a Péclet effect. *Oecologia* **138,** 426–435 (2004).

37. Al Charideh, A. R. & Abou Zakhem, B. Distribution of tritium and stable isotopes in precipitation in Syria. *Hydrol. Sci. J.* **55,** 832–843 (2010).

38. Bar-Matthews, M., Ayalon, A. & Kaufman, A. Late Quaternary paleoclimate in the eastern Mediterranean region from stable isotope analysis of speleothems at Soreq Cave, Israel. *Quat. Res.* **47,** 155–168 (1997).

39. Bajjali, W. Spatial variability of environmental isotope and chemical content of precipitation in Jordan and evidence of slight change in climate. *Appl. Water Sci.* **2,** 271–283 (2012).

40. Bowen, G., Wassenaar, L. & Hobson, K. Global application of stable hydrogen and oxygen isotopes to wildlife forensics. *Oecologia* **143,** 337–348 (2005).

41. Rozanski, K., Araguás-Araguás, L. & Gonfiantini, R. Isotopic patterns in modern global precipitation in *Climate Change in Continental Isotopic Records* (eds Swart, P. K., Lohmann, K. C., McKenzie, J. & Savin, S.) 1–36 (American Geophysical Union, 1993).

42. Gat, J. & Dansgaard, W. Stable isotope survey of the fresh water occurrences in Israel and the northern Jordan Rift Valley. *J. Hydrol.* **16,** 177–211 (1972).

43. Zaarur, S., Affek, H. & Stein, M. Last glacial–Holocene temperatures and hydrology of the Sea of Galilee and Hula Valley from clumped isotopes in *Melanopsis* shells. *Geochim. Cosmochim. Acta* **179,** 142–155 (2016).

44. Gat, J. Comments on the stable isotope method in regional groundwater investigations. *Water Resour. Res.* **7,** 980–993 (1971).

45. Farahani, A., Miller, M. J., Porter, B. W., Dawson, T. & Routledge, B. Stable isotopes of archaeological and modern semi-terrestrial crabs (*Potamon potamios*) provide paleoecological insights into brachyuran ecology and human resource acquisition in late Holocene Jordan. *Quat. Int.* **658,** 14–23 (2023).

46. Rozanski, K. Deuterium and oxygen-18 in European groundwaters—links to atmospheric circulation in the past. *Chem. Geol. Isot. Geosci. Sect.* **52,** 349–363 (1985).

47. Farquhar, G. & Richards, R. A. Isotopic composition of plant carbon correlates with water-use efficiency of wheat genotypes. *Aust. J. Plant Physiol.* **11,** 539–552 (1984).

48. Farquhar, G., Ehleringer, J. & Hubick, K. Carbon isotope discrimination and photosynthesis. *Annu. Rev. Plant Physiol. Plant Mol. Biol.* **40,** 503–537 (1989).

49. Ehleringer, J. & Cooper, T. Correlations between carbon isotope ratio and microhabitat in desert plants. *Oecologia* **76,** 562–566 (1988).

50. Hartman, G. & Danin, A. Isotopic values of plants in relation to water availability in the eastern Mediterranean region. *Oecologia* **162,** 837–852 (2010).

51. Körner, C., Farquhar, G. & Roksandic, Z. A global survey of carbon isotope discrimination in plants from high altitude. *Oecologia* **74,** 623–632 (1988).

52. Rudov, A., Mashkour, M., Djamali, M. & Akhani, H. A review of C_4 plants in southwest Asia: an ecological, geographical and taxonomical analysis of a region with high diversity of C_4 eudicots. *Front. Plant Sci.* **11,** 546518 (2020).

53. Arnold, E. R. et al. Provisioning the Early Bronze Age city of Tell es-Safi/Gath, Israel: isotopic analyses of domestic livestock management patterns. *Open Quat.* **4,** 1–12 (2018).

54. Mor, E., Greenberg, R. & Langgut, D. Paleoenvironment and fruit tree horticulture at Early Bronze Age Tel Bet Yerah: evidence from charcoal remains. *Bull. Am. Sch. Orient. Res.* **394,** 43–71 (2025).

55. Berger, A., Longford, C., Greenberg, R. & Fuller, D. Q. Archaeobotany at Tel Bet Yerah (Khirbet el-Kerak): aspects of food production in early urban and diasporic Early Transcaucasian communities of the Levant. *Environ. Archaeol.* https://doi.org/10.1080/14614103.2024.2434430 (2024).

56. Larson, K., Arnold, E. R. & Hardin, J. W. Resource allocation and rising complexity during the Iron Age IIA: an isotopic case study from Khirbet Summeily, Israel. *Quat. Int.* **646,** 68–80 (2023).

595 57. Louhaichi, M. & Tastad, A. The Syrian steppe: past trends, current status, and future priorities.
596 *Rangelands* **32,** 2–7 (2010).
597
598 58. Sadiddin, A. & Al Sayed, M. *Syrian Farming Systems: The Pastoral and the Agro-Pastoral*
599 *Farming Systems of the Semi-Arid and Arid Eastern Plains* (National Agricultural Policy Center,
600 2005).
601
602 59. Spiciarich, A. et al. Unveiling ancient Jerusalem's pastoral dynamics (7th to 2nd centuries BCE)
603 with multi-isotope analysis. *Sci. Rep.* **14,** 27278 (2024).
604
605 60. Vermeersch, S. et al. New insights into the diet and economy of the central and northern
606 Transjordan during the Iron Age: zooarchaeology and stable isotopes analysis of recent excavations
607 (Amman Citadel, Tell Zira'a, Tell Bleibil, and Tell Ushayer). *J. Archaeol. Sci. Rep.* **74,** 105990
608 (2026).
609
610 61. Bender, F. *Geology of Jordan* (Gebrüder Borntraeger, 1974).
611
612 62. Ponikarov, V. P. (ed.) *The Geology of Syria: Explanatory Notes on the Geological Map of Syria,*
613 *Scale 1:500,000* (Ministry of Industry, Syrian Arab Republic, 1967).
614
615 63. Sneh, A., Bartov, Y., Weissbrod, T. & Rosensaft, M. *Geological Map of Israel, Scale 1:200,000*
616 (Geological Survey of Israel, 1998).
617
618 64. Nicolle, C. Beyond urbanization, regional settlement pattern in south-eastern Levant during the
619 Early Bronze Age. *Levant* **55,** 26–45 (2023).
620
621 65. Maurer, G. et al. Seasonality and mobility: an integrative framework for reconstructing Kura-
622 Araxes pastoral systems at Maxta I, Nakhchivan. *PLoS ONE* **21,** e0346108 (2026).
623
624 66. Samei, S., Munro, N. D., Alizadeh, K. & Hartman, G. Highland pastoralism in the Early Bronze
625 Age Kura-Araxes cultural tradition: stable oxygen ($\delta^{18}O$) and carbon ($\delta^{13}C$) isotope analyses of herd
626 mobility at Köhne Shahar in northwestern Iran. *J. Archaeol. Sci. Rep.* **47,** 103773 (2023).
627
628 67. Greenberg, R. et al. The Circles Building (granary) at Tel Bet Yerah (Khirbet el-Kerak): a new
629 synthesis (excavations of 1945–1946, 2003–2015). *Bull. Am. Sch. Orient. Res.* **378,** 163–202 (2017).
630
631 68. Helmer, D. Biometria i arqueozoologia a partir d'alguns exemples del Pròxim Orient. *Cota Zero*
632 **11,** 51–60 (1995).
633
634 69. Jones, G. G. Variations of mandibular tooth accessory pillars, and metrical and morphological
635 differences between M1 and M2, in the cattle associated with the chariot burial (Appendix 11) in *The*
636 *Archaeology of the A1(M) Darrington to Dishforth DBFO Road Scheme* (eds Brown, F. C. et al.)
637 618–625 (Oxford Archaeology North, 2007).
638
639 70. Halstead, P., Collins, P. & Isaakidou, V. Sorting the sheep from the goats: morphological
640 distinctions between the mandibles and mandibular teeth of adult *Ovis* and *Capra*. *J. Archaeol. Sci.*
641 **29,** 545–553 (2002).
642

643 71. Tornero, C., Bălăşescu, A., Ughetto-Monfrin, J., Voinea, V. & Balasse, M. Seasonality and season
644 of birth in early Eneolithic sheep from Cheia (Romania): methodological advances and implications
645 for animal economy. *J. Archaeol. Sci.* **40,** 4039–4055 (2013).
646
647 72. Balasse, M. Reconstructing dietary and environmental history from enamel isotopic analysis: time
648 resolution of intra-tooth sequential sampling. *Int. J. Osteoarchaeol.* **12,** 155–165 (2002).
649
650 73. Suga, S. Progressive mineralization pattern of developing enamel during the maturation stage. *J.*
651 *Dent. Res.* **61,** 1532–1542 (1982).
652
653 74. Balasse, M. Potential biases in sampling design and interpretation of intra-tooth isotope analysis.
654 *Int. J. Osteoarchaeol.* **13,** 3–10 (2003).
655
656 75. Weinreb, M. M. & Sharav, Y. Tooth development in sheep. *Am. J. Vet. Res.* **25,** 891–908 (1964).
657
658 76. Noddle, B. Ages of epiphyseal closure in feral and domestic goats and ages of dental eruption. *J.*
659 *Archaeol. Sci.* **1,** 195–204 (1974).
660
661 77. Milhaud, G. & Nézit, J. Développement des molaires chez le mouton. Étude morphologique,
662 radiographique et microdurométrique. *Rec. Méd. Vét.* **167,** 121–127 (1991).
663
664 78. Zazzo, A. et al. The isotope record of short- and long-term dietary changes in sheep tooth enamel:
665 implications for quantitative reconstruction of paleodiets. *Geochim. Cosmochim. Acta* **74,** 3571–3586
666 (2010).
667
668 79. Brown, W. A. B., Christofferson, P. V., Massler, M. & Weiss, M. B. Postnatal tooth development
669 in cattle. *Am. J. Vet. Res.* **21,** 7–34 (1960).
670
671 80. Andrews, A. The relationship of bovine mandibular cheek tooth development to age determined
672 by post-mortem radiographic examination of cattle aged between 12 and 24 months. *J. Agric. Sci.* **98,**
673 109–117 (1982).
674
675 81. Cerling, T. & Harris, J. Carbon isotope fractionation between diet and bioapatite in ungulate
676 mammals and implications for ecological and paleoecological studies. *Oecologia* **120,** 347–363
677 (1999).
678
679 82. Passey, B. H. et al. Carbon isotope fractionation between diet, breath CO_2, and bioapatite in
680 different mammals. *J. Archaeol. Sci.* **32,** 1459–1470 (2005).
681
682 83. Balasse, M., Obein, G., Ughetto-Monfrin, J. & Mainland, I. Investigating seasonality and season
683 of birth in past herds: a reference set of sheep enamel stable oxygen isotope ratios. *Archaeometry* **54,**
684 349–368 (2012).
685
686 84. Balasse, M., Tresset, A., Dobney, K. & Ambrose, S. H. The use of isotope ratios to test for
687 seaweed eating in sheep. *J. Zool.* **266,** 283–291 (2005).
688

85. Balasse, M. et al. Neolithic sheep birth distribution: results from Nova Nadezhda (sixth millennium BC, Bulgaria) and a reassessment of European data with a new modern reference set including upper and lower molars. *J. Archaeol. Sci.* **118,** 105139 (2020).

86. Balasse, M., Chemineau, P., Parisot, S., Fiorillo, D. & Keller, M. Experimental data from Lacaune and Merino sheep provide new methodological and theoretical grounds to investigate autumn lambing in past husbandries. *J. Archaeol. Method Theory* **31,** 75–92 (2024).

87. Blaise, E. & Balasse, M. Seasonality and season of birth of modern and Late Neolithic sheep from south-eastern France using tooth enamel $\delta^{18}O$ analysis. *J. Archaeol. Sci.* **38,** 3085–3093 (2011).

88. Tornero, C. et al. Vertical sheep mobility along the altitudinal gradient through stable isotope analyses in tooth molar bioapatite, meteoric water and pastures: a reference from the Ebro Valley to the Central Pyrenees. *Quat. Int.* **484,** 94–106 (2018).

89. Batiuk, S. Migration theory and the distribution of the Early Transcaucasian culture. PhD thesis, Univ. Toronto (2005).

90. Balasse, M. et al. Seasonal calving in European prehistoric cattle and its impacts on milk availability and cheese-making. *Sci. Rep.* **11,** 8185 (2021).

Acknowledgements

This project was funded by the London Arts & Humanities Partnership (LAHP) and the Israel Science Foundation (grant no. 681/19).

Author Contributions:

GM – Conceptualisation, Data curation, Formal analysis, Investigation, Methodology, Software, Visualisation, Writing – original draft, Writing – review & editing. RG – Conceptualisation, Funding acquisition, Project administration, Resources, Supervision, Validation, Writing – original draft, Writing – review & editing. DF – Investigation, Methodology, Validation, Writing – original draft, Writing – review & editing. AN – Formal analysis, Methodology, Validation. RS – Investigation, Methodology, Supervision, Validation, Writing – review & editing.

Additional information

Competing interests:

The authors declare no competing interests.

Figure legends

Figure 1. Map of Khirbet Kerak Ware (KKW) sites in the Levant. Site coordinates after Batiuk [89]. Temporal association of samples after Regev et al. [20]. Shaded areas indicate hypothetical KKW winter–spring pasture zones. The Mediterranean C_3 line marks the approximate extent of C_3-dominated Mediterranean vegetation, while the Badiya line represents the approximate 200 mm mean annual rainfall isohyet, commonly used to delimit the arid Badiya from wetter areas to the west. Coordinates of sites are available in Supplementary Table S1.

Figure 2. A model of KKW and Levantine livestock herding strategies. (a) Annual husbandry calendar contrasting Local agro-integrated management (including seasonal use of post-harvest fields) with KKW seasonal use of winter pastures in a C_3/C_4 ecotone and summer grazing in predominantly C_3 Mediterranean settings. (b) Schematic ecological gradient showing the expected direction of dietary $\delta^{13}C$ change with increasing C_4 availability/aridity. (c) Hypothetical stable isotope values of sequential samples of enamel bioapatite from cattle, sheep and goat molars under each strategy.

Figure 3. Minimum, mean and maximum of sequential stable $\delta^{18}O$ and $\delta^{13}C$ isotope values. Only specimens with clear maxima and minima are shown: sheep (*Ovis*) – TBY70203, TBY702805, TBY70145, TBY70656 and TBY70168; goat (*Capra*) – TBY70158, TBY70444 and TBY70647; sheep/goat (*Ovis/Capra*) – TBY702839 and TBY70489; cattle (*Bos*) – TBY37, TBY702849 and TBY70316. Specimen without an icon represent sheep/goat. Panels were annotated and assembled in Adobe Illustrator V. 2026. Sheep, goat and cattle icons from Vecteezy.com.

Figure 4. Sequential stable $\delta^{13}C$ (red) and $\delta^{18}O$ (black) isotope profiles plotted against distance from the root-enamel junction for caprines and cattle. The shaded $\delta^{18}O$ envelope indicates a bootstrapped 95% confidence interval from a cosine model fit (n = 600). Axes are reversed to reflect enamel mineralization direction. Wet C_3 and dry C_3 are based on wet- and dry-season plant values from Hartman and Danin [50], used here to represent fresher and more water-stressed C_3 forage, respectively. The figure was annotated and assembled in Adobe Illustrator V. 2026. Sheep, goat and cattle icons from Vecteezy.com.

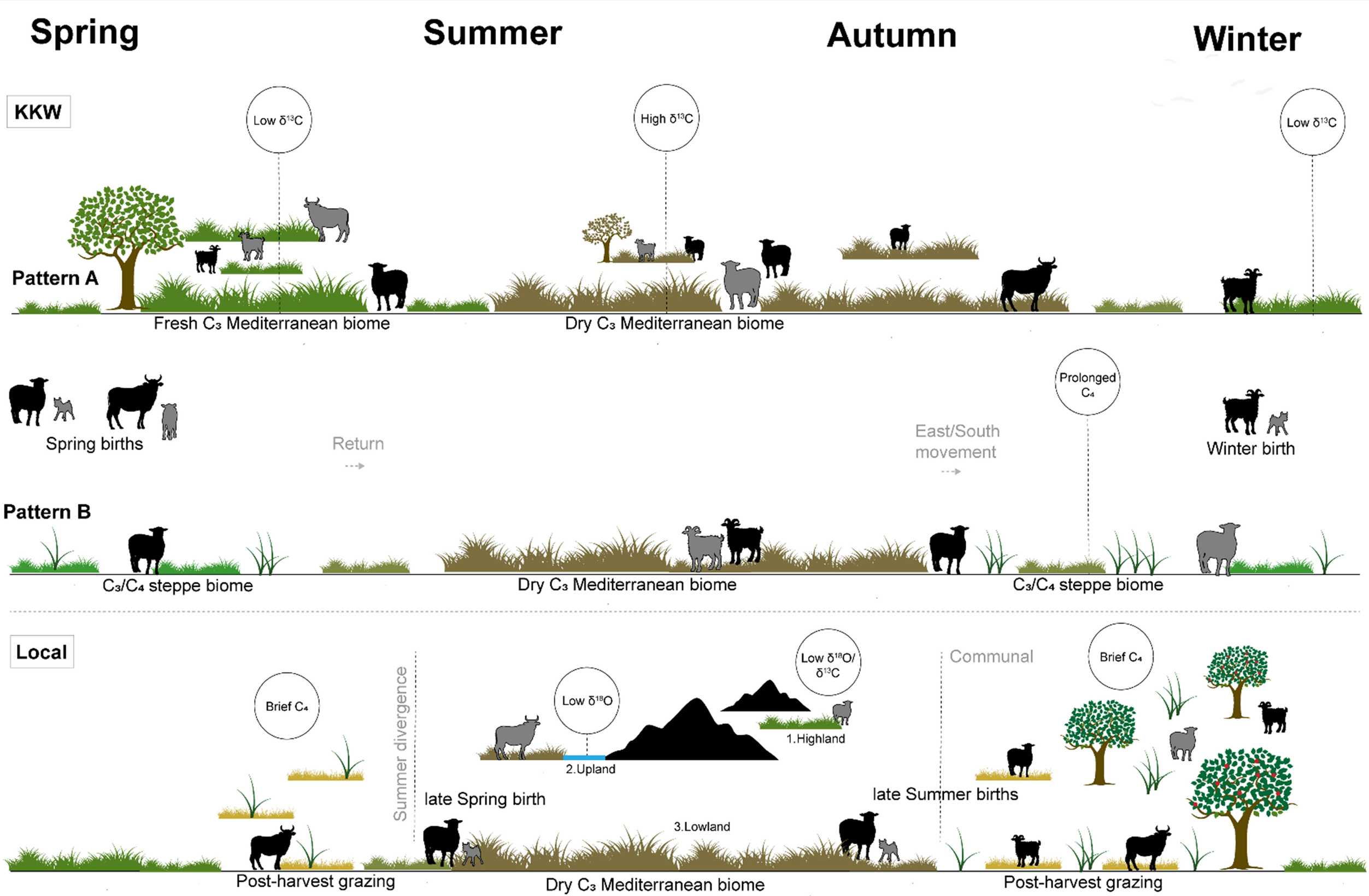
Figure 5. Seasonality of sheep, goat and cattle births at Tel Bet Yerah inferred from normalised maximum $\delta^{18}O$ values in tooth crowns (x_0/X), compared with modern reference datasets [83,85–88,90] (D. Frémondeau, unpublished data). Shaded areas

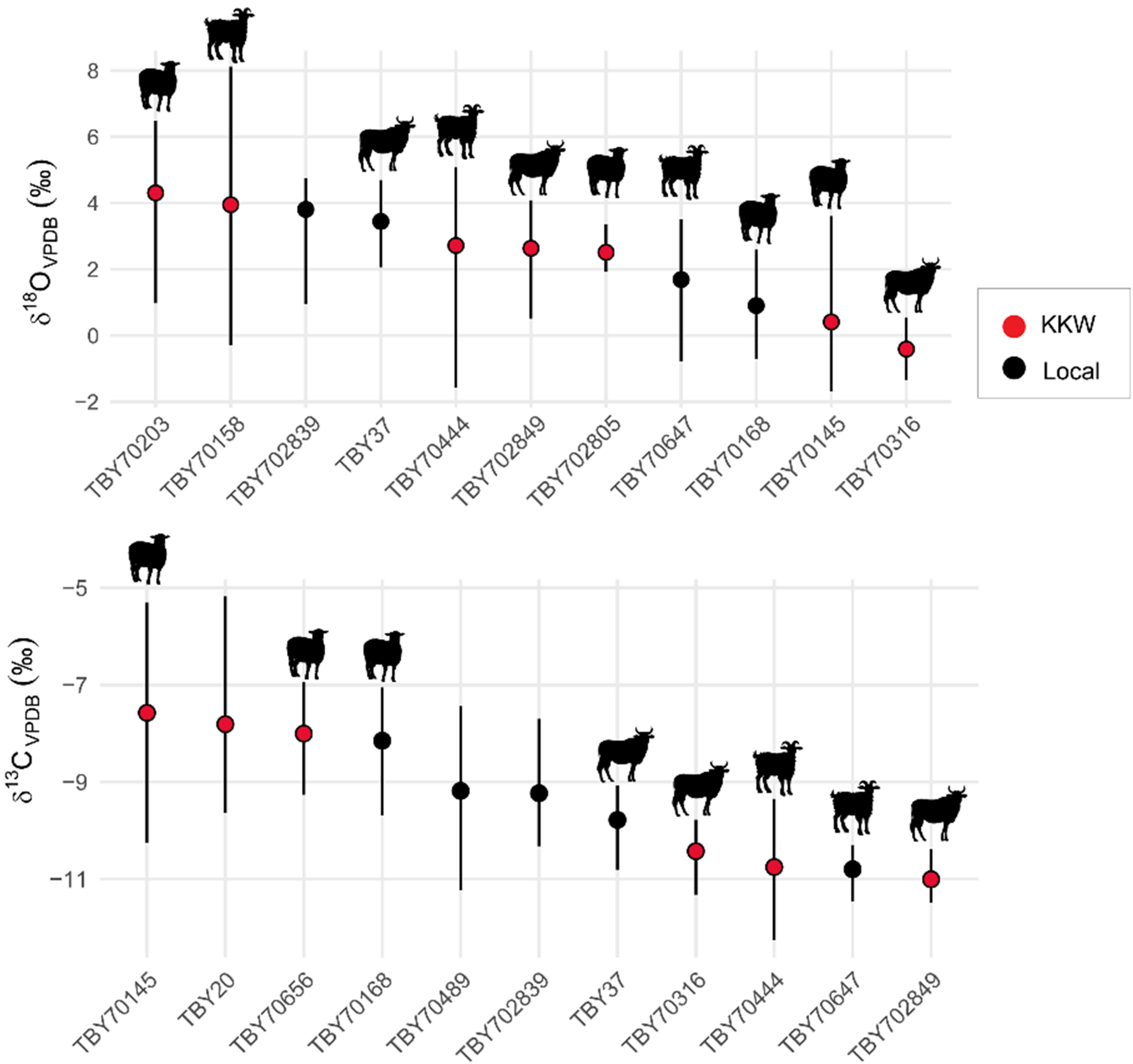
764 indicate modern seasonal ranges; red dots show KKW specimens and black dots local
765 specimens. Details in Supplementary Table S3c.
766
767 **Figure 6. Sheep and goat grazing on post-harvest fields with dry C_3 stubble and C_4**
768 **weeds in the Sulaymaniyah province, Iraqi Kurdistan.** Image taken by the author in
769 October 2023.
770
771
772
773
774
775 **Table 1. Specimen-level summary statistics for sequential enamel $\delta^{18}O$ and $\delta^{13}C$ values**
776 **from caprines and cattle at Tel Bet Yerah (Khirbet-el-Kerak), including minimum,**
777 **mean, maximum and intra-tooth amplitude values. Tooth wear stages (TWS) are**
778 **according to Grant 1982.** The full sequential isotope dataset is provided in Supplementary
779 Data S3.

Specimen	Taxa	Tooth	TWS	Phase	n	$\delta^{18}O$ mean	$\delta^{18}O$ min	$\delta^{18}O$ max	$\delta^{18}O$ range	$\delta^{13}C$ mean	$\delta^{13}C$ min	$\delta^{13}C$ max	$\delta^{13}C$ range
TBY20	*Ovis/capra*	M/2		KKW	12	3.7	2.4	5.0	2.7	-7.8	-9.6	-5.2	4.5
TBY70145	*Ovis*	M/2	f	KKW	13	0.4	-1.7	3.6	5.3	-7.6	-10.3	-5.3	5.0
TBY70157	*Capra*	M/2	e	KKW	12	1.6	0.5	3.5	3.0	-7.3	-10.3	-5.6	4.7
TBY70158	*Capra*	M/2	g	KKW	9	4.0	-0.3	8.1	8.4	-9.7	-10.7	-8.9	1.9
TBY70203	*Ovis*	M/2	g	KKW	8	4.3	1.0	6.5	5.5	-10.8	-11.5	-10.2	1.3
TBY70444	*Capra*	M/2	e	KKW	10	2.7	-1.6	5.1	6.7	-10.8	-12.3	-9.3	2.9
TBY70656	*Ovis*	M/2	h	KKW	9	2.4	1.8	3.1	1.3	-8.0	-9.3	-6.9	2.3
TBY702805	*Ovis*	M/2	g	KKW	8	2.5	1.9	3.3	1.4	-8.4	-9.6	-7.2	2.4
TBY70489	*Ovis/capra*	M/2	g	EB3 early	11	1.9	0.2	3.2	3.0	-9.2	-11.2	-7.4	3.8
TBY70168	*Ovis*	M/2	g	EB3 local	9	0.9	-0.7	2.6	3.3	-8.1	-9.7	-7.1	2.6
TBY70652	*Capra*	M/2	f	EB3 local	9	2.2	0.2	2.3	2.2	-7.2	-8.5	-6.5	2.0
TBY70647	*Capra*	M/2	f	EB2 latest	14	1.7	-0.8	3.5	4.3	-10.8	-11.5	-10.3	1.2
TBY702839	*Ovis/capra*	M/2		EB2 latest	14	3.8	0.9	4.8	3.8	-9.2	-10.3	-7.7	2.6
TBY702849	*Bos*	M/3	l	KKW	14	2.6	0.5	4.1	3.6	-11.0	-11.5	-10.4	1.1
TBY45	*Bos*	M/3		KKW	16	-0.8	-1.6	0.5	2.1	-10.1	-10.7	-9.3	1.4
TBY70316	*Bos*	M/3	f	KKW	12	-0.4	-1.3	0.5	1.9	-10.4	-11.3	-9.8	1.5
TBY39	*Bos*	M/3		EB3 local	18	-2.2	-3.9	-0.5	3.3	-9.6	-10.1	-9.2	0.9
TBY702827	*Bos*	M/3	g	EB2 Late	14	0.9	-0.8	1.7	1.7	-7.9	-9.3	-6.0	3.3
TBY37	*Bos*	M/3		EB2	15	3.4	2.1	4.7	2.6	-9.8	-10.8	-9.1	1.7

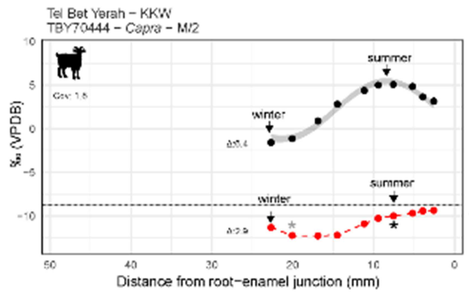
780
781

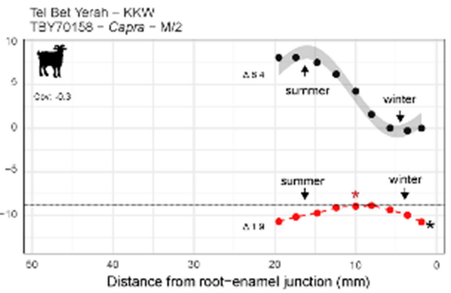
KKW producing sites
KKW sherds identified
1 Tel Bet Yerah / Khirbet el-Kerak
2 Tel Qishyon / Tell Kasyun
3 Tel Yaqush
4 Tell esh-Shuna
5 Bet Shan / Beit Shean
6 Tel Hazor
Mediterranean C_3 vegetation
Badiya
hypothetical KKW winter-spring pasture
100 km
Amuq plain
Lebanon Mountains
Anti-Lebanon Mountains
Jordan River
Galilee
Jezreel
36°N
34°N
32°N
30°N
34°E
36°E
38°E
40°E
Samples from Tel Bet Yerah (Khribet-el-Kerak)
TBY39
TBY70652
TBY70329
TBY70168
TBY20
TBY702849
TBY702805
TBY70656
TBY70444
TBY70316
TBY70203
TBY70158
TBY70157
TBY45
TBY70145
TBY70489
TBY702839
TBY70647
TBY702827
TBY9990333
TBY37
3300
3100
2900
2700
2500
cal BC
KKW
Local

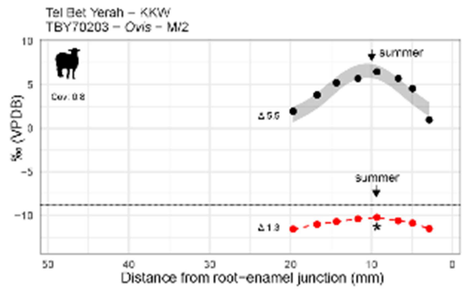

Spring
Summer
Autumn
Winter
KKW
Low δ13C
High δ13C
Low δ13C
Pattern A
Fresh C3 Mediterranean biome
Dry C3 Mediterranean biome
Spring births
Return
East/South movement
Prolonged C4
Winter birth
Pattern B
C3/C4 steppe biome
Dry C3 Mediterranean biome
C3/C4 steppe biome
Local
Brief C4
Summer divergence
Low δ18O
Low δ18O/ δ13C
1.Highland
2.Upland
3.Lowland
late Spring birth
late Summer births
Communal
Brief C4
Post-harvest grazing
Dry C3 Mediterranean biome
Post-harvest grazing


δ18OVPDB (‰)
8
6
4
2
0
−2
TBY70203
TBY70158
TBY702839
TBY37
TBY70444
TBY702849
TBY702805
TBY70647
TBY70168
TBY70145
TBY70316
KKW
Local
δ13CVPDB (‰)
−5
−7
−9
−11
TBY70145
TBY20
TBY70656
TBY70168
TBY70489
TBY702839
TBY37
TBY70316
TBY70444
TBY70647
TBY702849

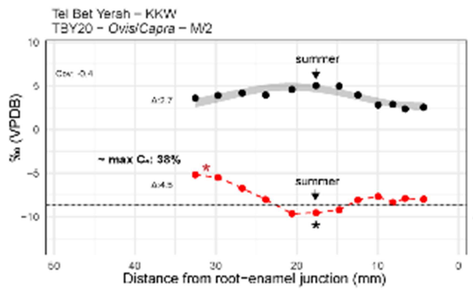
Pattern A - KKW

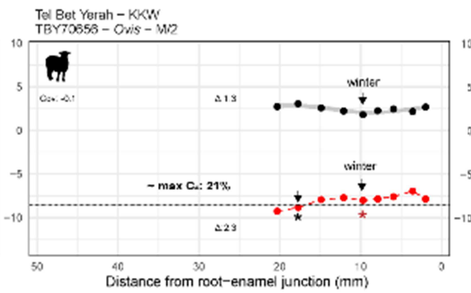


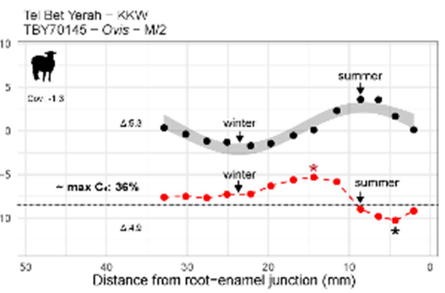


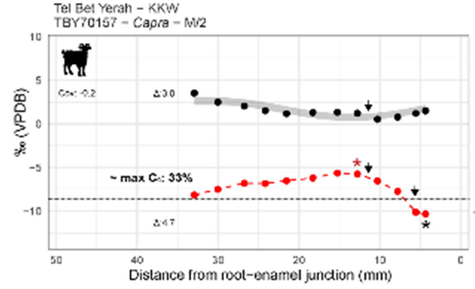


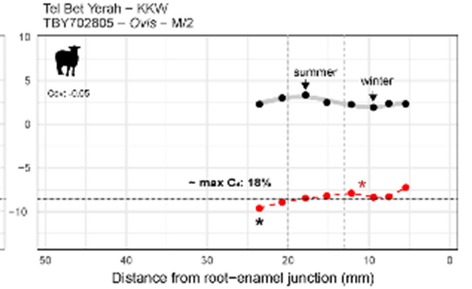
Pattern B - KKW



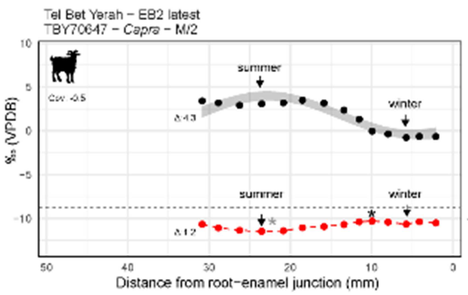


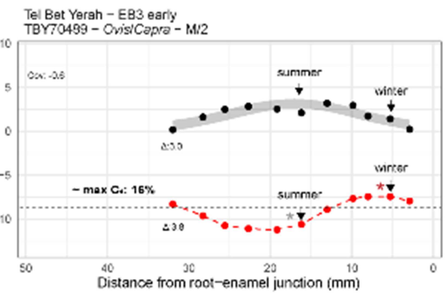




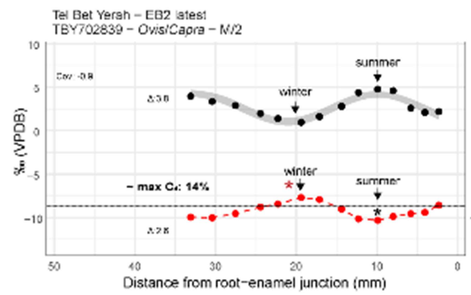


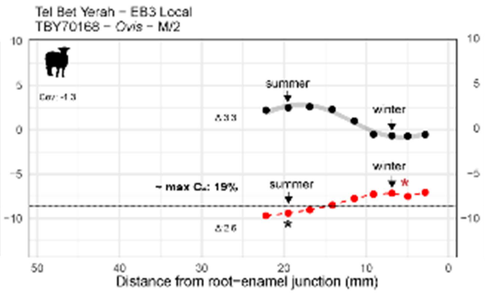
Pattern C - Local

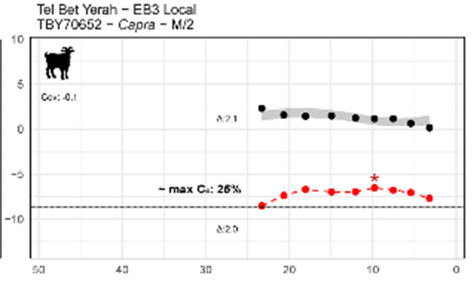




Pattern D - Local

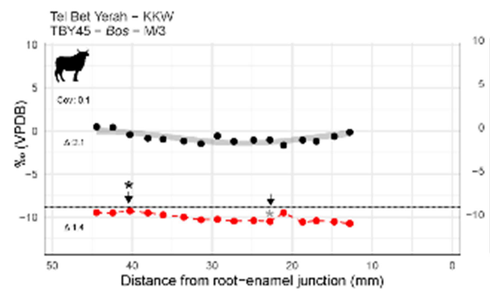


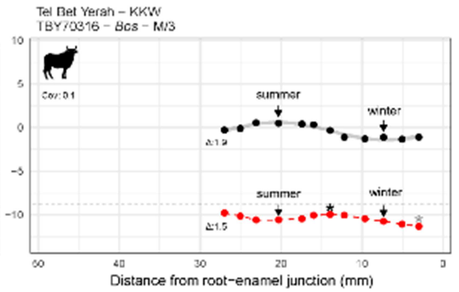




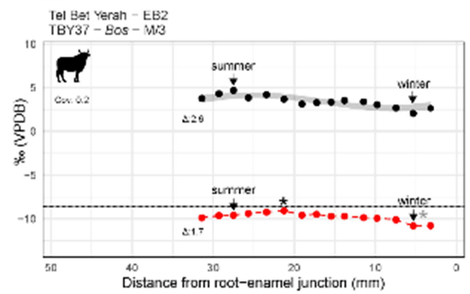
Pattern E - KKW & Local

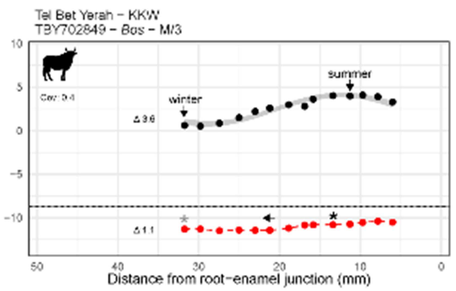
E.1



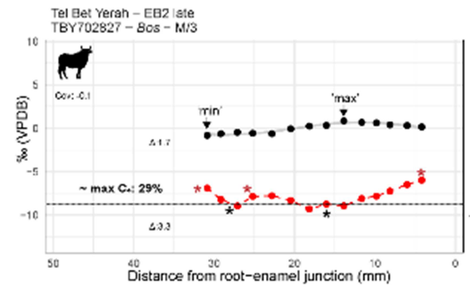


E.2

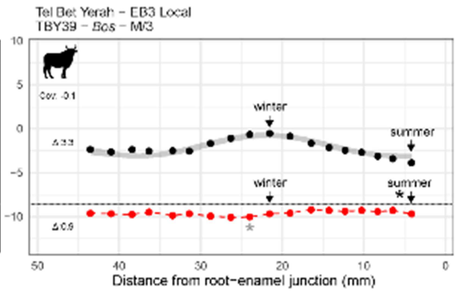


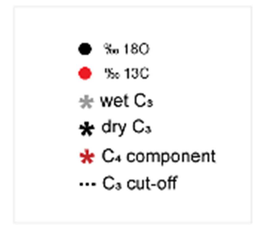


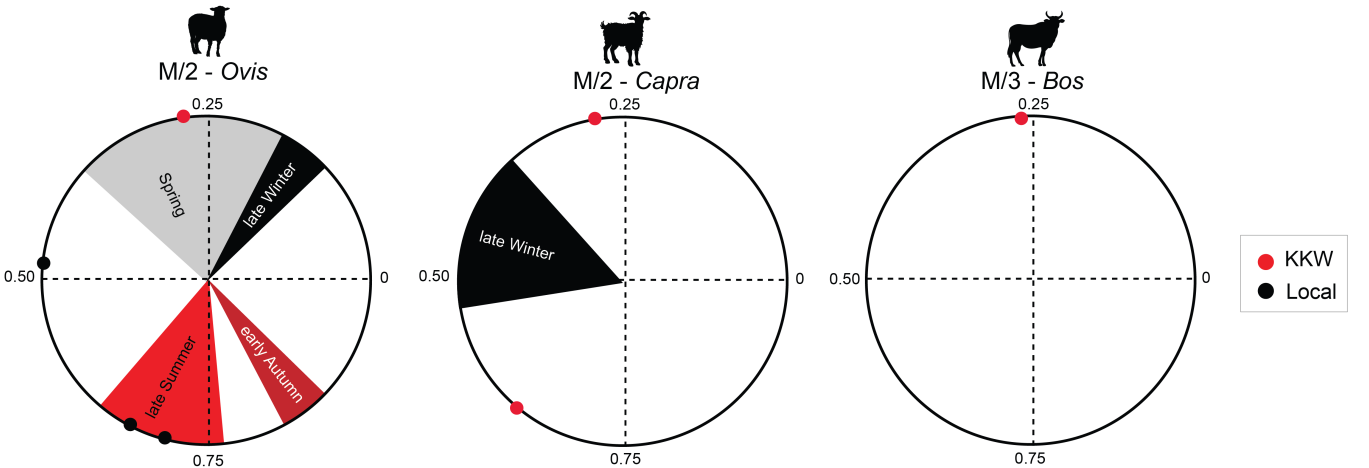
Pattern F - Local



Pattern G - Local






M/2 - Ovis
0.25
0.50
0
0.75
Spring
late Winter
late Summer
early Autumn
M/2 - Capra
0.25
0.50
0
0.75
late Winter
M/3 - Bos
0.25
0.50
0
0.75
KKW
Local



Supplementary Files

This is a list of supplementary files associated with this preprint. Click to download.

- Supplementarymaterial.zip